# Insights into the $H_2O/V_2O_5$ Interface Structure for Optimizing Water-splitting①

ZHANG Bing-Kai[a, b] LI Zeng-Zhu[a] LI Qiong[a]
LIN Zhan[a②] LIU Jing[c②] PAN Feng[b②]
[a] (*School of Chemical Engineering and Light Industry, Guangdong University of Technology, Guangzhou* 510006, *China*)
[b] (*School of Advanced Materials, Peking University, Shenzhen Graduate School, Shenzhen* 518055, *China*)
[c] (*State Key Laboratory of Coal Combustion, Huazhong University of Science and Technology, Wuhan* 430074, *China*)

**ABSTRACT** The interaction of water ($H_2O$) with metal oxide surfaces is of fundamental importance to various fields of science, ranging from batteries to catalysis. In particular, vanadium pentoxide ($V_2O_5$) has been widely used as electrode materials for aqueous-battery and catalysts. Herein, theoretical (density functional theory) study gives atomic-scale insights into water monolayers in $V_2O_5$ and single-molecule adsorption and dissociation at three low-index surfaces and oxygen-vacancy $V_2O_5$(001) surface. The $H_2O/V_2O_5$ interface structure was identified. The results show that $H_2O$ is adsorbed on the stoichiometric $V_2O_5$(001) surface with physisorption mechanism, and the dissociation hardly occurs. Water adsorbs as an intact monomer with a computed binding energy of 0.75 eV. The formation of ordered water overlayers has been observed on $V_2O_5$(001) surface, suggesting a locally ordered superstructure of molecular water. The molecular $H_2O$ adsorption on oxygen-vacancy $V_2O_5$(001) surface is stronger than that on the stoichiometric $V_2O_5$(001) surface, and $H_2O$ can undergo dissociative chemisorption to form a surface hydroxyl group and a H adatom. $V_2O_5$ can take the oxygen from $H_2O$, which is consistent with the experimental results.

**Keywords: $V_2O_5$, interface structure, adsosption, dissociation, density functional calculations;**
**DOI: 10.14102/j.cnki.0254–5861.2011–2748**

## 1 INTRODUCTION

Water ($H_2O$) is one of the most studied adsorbates on well-defined metal oxide single crystal samples. The adsorption of $H_2O$ at solid surfaces shows a variety of applications in electrochemistry (The formation of water molecules near a metal electrode plays a key role in electrochemical reactions) and in heterogeneous catalysis[1-3]. It has been generally accepted that the interaction of $H_2O$ with metal oxide surfaces has important consequences on their catalytic behaviors. The adsorption of $H_2O$ on a metal oxide

Received 25 January 2020; accepted 3 February 2020
① This work was financially supported by startup R&D funding from the One-Hundred Young Talents Program of Guangdong University of Technology (No. 22041331901), National Key R&D Program of China (2016YFB0700600), Soft Science Research Project of Guangdong Province (No. 2017B030301013), and Shenzhen Science and Technology Research Grant (ZDSYS201707281026184)
② Corresponding authors. Lin Zhan, E-mail: zhanlin@gdut.edu.cn; Liu Jing, E-mail: liujing@mail.hust.edu.cn; Pan Feng, E-mail: panfeng@pkusz.edu.cn

surface may result in different adsorption modes, or combinations of them, depending on the measurement temperature, the intrinsic reactivity of the surface, and the number of oxygen-vacancy sites on the surface.

Vanadium pentoxide ($V_2O_5$) is an important transition metal oxide and has been widely used as electrode materials for rechargeable aqueous Zn-ion battery and catalysts in many industrial applications[4-6]. Since Zn-ion storage and heterogeneous catalytic reactions take place in aqueous solutions or in a humid environment, it is significant to understand the interaction mechanisms of $H_2O$ on $V_2O_5$. Meanwhile, in the application of photocatalysis, water not only provides the reaction environment but also is the key participant, as it can decompose to produce hydrogen, oxygen, and hydroxyl radicals. Therefore, a detailed investigation of $H_2O$ adsorption and dissociation on $V_2O_5$ surfaces is also very important, which can help to elucidate the mechanism of catalytic processes occurring on $V_2O_5$ catalyst.

Experimental studies based on Fourier transform infrared (FTIR) spectroscopy showed that $H_2O$ is adsorbed on unsupported $V_2O_5$ and surface metal centers acting as Lewis acids are the favorable sites[7, 8]. Costa et al. observed that water is molecularly adsorbed on $V_2O_5$(001) based on the observation of the ambient atomic force microscopy on $V_2O_5$(001) surface[9]. Moshfegh et al. have carried out temperature programmed desorption (TPD) studies and found that $H_2O$ adsorbs dissociatively on the $V_2O_5$ surface through the action of two neighboring vanadium sites of $-V^{5+}$-O-$V^{4+}$[10]. The analyis results of some important reactions show that the structures of surface $V_2O_5$/supports are generally altered in the presence of water, and water effect is connected with the formation of the Brönsted acids V-OH. Sadovskaya et al.[11] and Lee et al.[12] proposed that the lattice oxygen of surface vanadia species $VO_x$ undergoes isotope exchange with that of adsorbed water rather than gas-phase oxygen. Recently, Ma et al.[13] have studied the reactions of vanadium oxide cluster cations with heavy water ($D_2O$) in a fast flow reactor. Their results suggested that $(V_2O_5)_{1\text{-}3}^+$ clusters are reactive toward water resulting in $(V_2O_5)_{1\text{-}3}D^+$ and $(V_2O_5)_{1\text{-}3}D_2O^+$ through the deuterium atom abstraction and adsorption reactions. The work of Goclon et al. showed that under low value of the oxygen partial pressure conditions, the $V_2O_5$ phase is unstable and may form oxygen-vacancy surface that is more active than stoichiometric $V_2O_5$ surface[14].

Compared to experimental works, the computational chemistry methodologies have been used to give further insight into the structural, electronic, magnetic and catalytic properties of the $V_2O_5$ surfaces, but the theoretical studies for $H_2O/V_2O_5$ interfaces and $H_2O/V_2O_5$ interactions are relatively limited. Yin et al.[15] and Witko et al.[16] studied the adsorption and dissociation of water at low-index $V_2O_5$ surfaces by cluster models. However, they did not study the water monolayers with $V_2O_5$ and a systematical investigation of adsorption and dissociation of water on different $V_2O_5$ surfaces including oxygen-vacancy surface by periodic density functional theory. In this study, the first-principles calculations based on density functional theory and the periodic slab models are used to investigate water monolayers with $V_2O_5$ and single-molecule adsorption and dissociation at three low-index surfaces ((001), (010) and (100)) of $V_2O_5$ and oxygen-vacancy $V_2O_5$(001) surface.

## 2 COMPUTATIONAL METHODS

Geometry optimizations and density of states calculations were performed using the Cambridge Serial Total Energy package (CASTEP)[17]. CASTEP is a first principles density functional theory plane wave pseudopotential simulation code. The calculations were performed in the frame of the generalized gradient approximation (GGA, Perdew-Burke-Enzerhoff (PBE)) for the exchange and correlation effects[18, 19]. Ultrasoft pseudopotentials corresponding to the optimization scheme of Vanderbilt were employed[20]. Surfaces were simulated by slabs separated by a vacuum region (14 Å). The cutoff energy is 380 eV. The number of k-points for Brillouin-Zone integration (BZ) was chosen accor-

ding to the Monkhorst-Pack scheme[21]. For bulk $V_2O_5$, a 5 × 5 × 5 k-points mesh was used, whereas for the supercells representing (001), (010), (100) and defective surfaces 4 × 4 × 1 grids were applied. All atoms in the three surfaces were allowed to relax. The convergence criteria for the structure optimization and energy calculation were set to (a) a SCF tolerance of $2.0 \times 10^{-6}$ eV/atom, (b) an energy tolerance of $2.0 \times 10^{-5}$ eV/atom, (c) a maximum force tolerance of 0.05 eV/Å, and (d) a maximum displacement tolerance of 0.002 Å. Spin-polarized calculations were also included in the DFT investigations. We have considered the effect of Hubbard U on the adsorption energies of water on $V_2O_5$(001) surface, and found that the effect is small (less than 1 kJ/mol), so the Hubbard U parameter was not included in the calculations.

$V_2O_5$ is a layerlike material with a no-covalent interaction between layers, making it easy for cleavage along the (001) plane, as shown in Fig. 1. $V_2O_5$ is an orthorhombic lattice (space group *Pmmn*) and its optimized unit cell parameters ($a$ = 11.512, $b$ = 3.564, $c$ = 4.368 Å) are within +0.2%, +0.1% and –2.8% errors, respectively of the experimental determined lattice constants[22], suggesting that the calculations are reliable. Three possible low-index surfaces of $V_2O_5$, namely the (010), (001) and (100), are shown in Fig. 2. In this work, two layers of $V_2O_5$ are used in the (001), (100), (010) and oxygen-vacancy (001) surfaces.

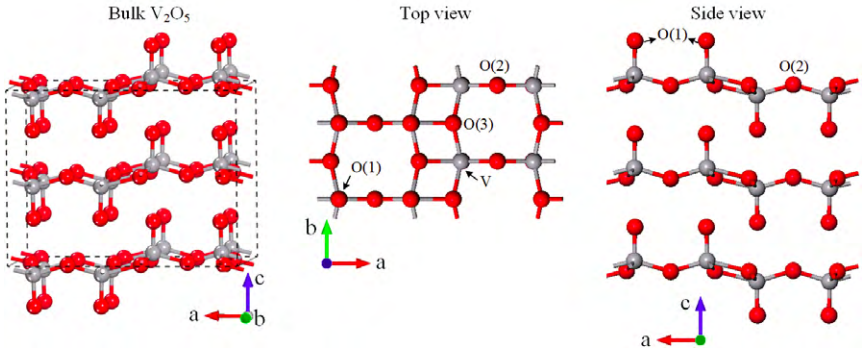


**Fig. 1. Crystal structure of $V_2O$ (Red and grey spheres are O and V atoms, respectively)**

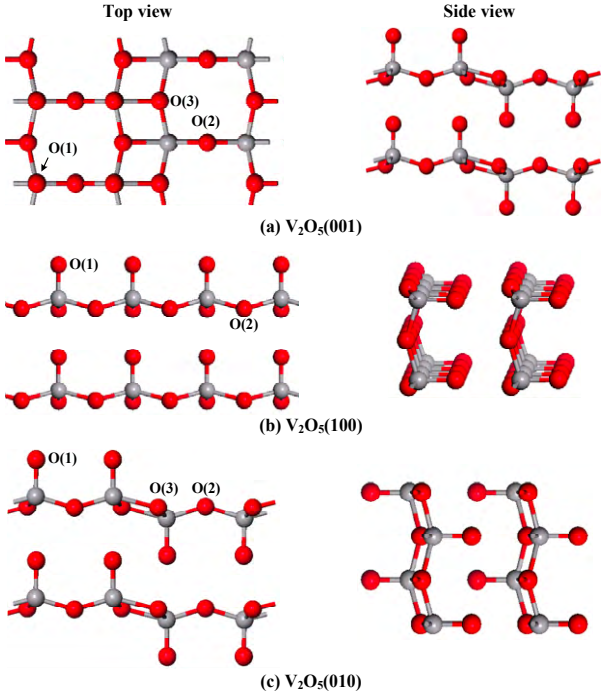


**Fig. 2. Three low-index surfaces of $V_2O_5$. (a) $V_2O_5$(001), (b) $V_2O_5$(100), and (c) $V_2O_5$(010) (Red spheres are O atoms and the gray ones are V atoms)**

There are three types of oxygen atoms differing by their coordination number with the vanadium atoms: (i) singly coordinated terminal oxygen, O(1), which is a vanadyl oxygen (V=O); (ii) two-coordinated oxygen, O(2); and (iii) three-coordinated oxygen, O(3). The O(2) and O(3) bridge two and three vanadium atoms, respectively.

For the adsorption of water molecule, 5-fold coordinated vanadium atoms and the surface oxygen atoms are the active sites. 5-Fold coordinated vanadium atoms are considered as Lewis acid site, which can interact with oxygen atom ($O_w$) of water with free electron pairs. Oxygen atoms at the surface can interact with hydrogen atoms of water through hydrogen bonds. For the adsorption of $H_2O$, both vanadium and oxygen sites of $V_2O_5$ surfaces are considered.

The adsorption energy ($E_{ads}$) has been calculated according to the expression:

$$E_{ads} = E_{(adsorbate\text{-}substrate)} - (E_{adsorbate} + E_{substrate}), \quad (1)$$

where $E_{(adsorbate\text{-}substrate)}$ is the total energy of the adsorbate/substrate system, $E_{adsorbate}$ is the total energy of the isolated adsorbate at its equilibrium geometry, and $E_{substrate}$ is the total energy of the substrate. A negative $E_{ads}$ value corresponds to a stable adsorbate/substrate system.

All transition states (TSs) are located by using the complete LST/QST method[23-25]. It starts with linear synchronous transit (LST) maximization, followed by energy minimization in directions conjugated to the reaction pathway. These approximated TS are then used to perform quadratic synchronous transit (QST) maximization. From that point, another conjugate gradient minimization is performed. The cycle is repeated until a stationary point is located. A transition state is identified when (1) the forces on the atoms vanish and (2) the energy is a maximum along the reaction coordinate but a minimum with respect to all of the other degrees of freedom. The energy barrier is the energy difference between the transition state (TS) and the intermediate (IM).

## 3 RESULTS AND DISCUSSION

### 3.1 $H_2O/V_2O_5$ interface structures and adsorption of $H_2O$ on the stoichiometric $V_2O_5$(001) surface

Firstly, the adsorption of $H_2O$ on the $V_2O_5$(001) surface was considered since the $V_2O_5$(001) surface is the thermodynamically most stable[26]. $H_2O$ is initially placed on different adsorption sites, i.e., O(1), O(2), O(3) and V on the $V_2O_5$ surface, as shown in Fig. 3. In the calculation process, all possible adsorption orientations were considered including parallel and vertical (O-down and H-down modes) to get all possible adsorption models for water on surfaces. The final stable configurations are obtained on the surface for each parallel and vertical orientations. The calculated adsorption energies and bond lengths for stable configurations are listed in Table 1.

**Table 1. Optimized Parameters for $H_2O$ Adsorption on the $V_2O_5$(001) Surface**

| Sites | $E_{ads}$ (kJ/mol) | $R_{surface\text{-}H_2O}$ (Å) | $R_{Ow\text{-}H}$ (Å) | $\theta_{H\text{-}Ow\text{-}H}$ (°) | $Q_{H_2O}$ (e) | $M_{surface\text{-}H_2O}$ |
|---|---|---|---|---|---|---|
| O(1) | –15.60 | 2.231 | 0.978/0.978 | 106.8 | 0.01 | 0.03 |
| O(2) | –14.33 | 2.240 | 0.978/0.976 | 105.9 | 0.00 | 0.02 |
| O(3) | –8.01 | 3.010 | 0.981/0.981 | 105.2 | 0.00 | 0.00 |
| V | –14.53 | 2.674 | 0.980/0.980 | 107.1 | 0.02 | 0.04 |

$E_{ads}$ denotes adsorption energies. $R$ is bond length. For O(1), O(2), and O(3) sites, the $R_{surface\text{-}H_2O}$ means the distance between surface O atoms and H atom of $H_2O$. For V site, the $R_{surface\text{-}H2O}$ stands for the distance between surface V atoms and $O_w$ atom of $H_2O$. $R_{Ow\text{-}H}$ represents the two bond lengthes of adsorbed $H_2O$. $Q$ shows charge transfer from $H_2O$ to surface. And $M$ denotes the bond population.

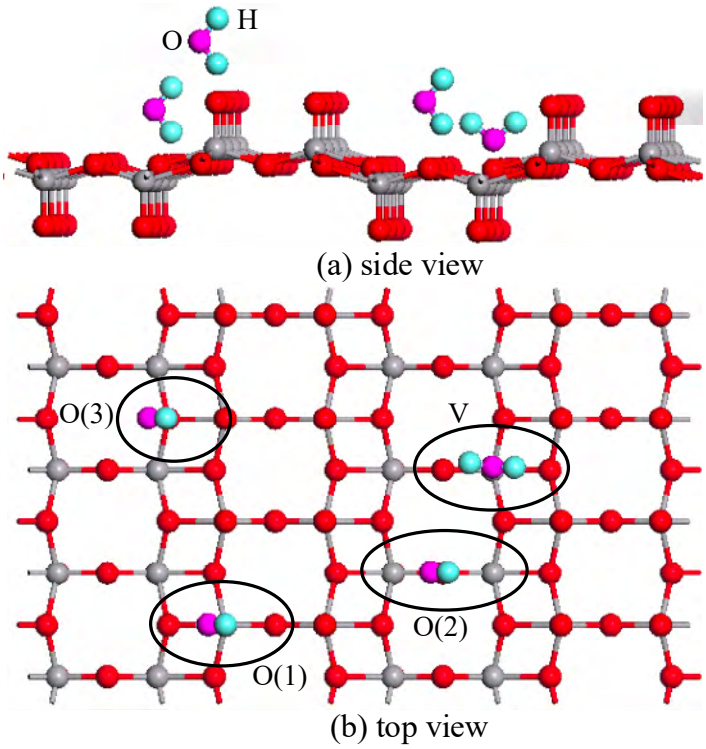


**Fig. 3. Scheme view of the four studied cases of $H_2O$ adsorption on $V_2O_5$(001) surface. (a) Side view and (b) Top view. Three different oxygen atoms and surface V atoms are available for reactivity (Red spheres: O atoms, gray spheres: V atoms, purple spheres: $O_w$ atoms of $H_2O$, and blue spheres: H atoms)**

The adsorption energies are in the range of –8.01 to –15.60 kJ/mol, and adsorption abilities decrease in the order of O(1) > V ≈ O(2) > O(3). The surface-$H_2O$ distances are changing from 2.231 to 3.010 Å. The highest adsorption energy of $H_2O$ calculated was –15.60 kJ/mol, which constitutes a weak interaction. The O(3) site is inactive with adsorption energy of –8.01 kJ/mol, which is different and is roughly 7.39 kJ/mol. The adsorption mechanism of $H_2O$ on stoichiometric $V_2O_5$(001) surface is physisorption. The Mulliken population analysis is performed to understand the charge trend between adsorbate and substrate. As listed in Table 1, the Mulliken charges for adsorbed $H_2O$ in the four adsorption configurations are below 0.02 e, suggesting few electrons withdrawing from $H_2O$ to the surface during adsorption. The bond populations between surface and $H_2O$ are almost zero. The above analyses suggest that the adsorption of water on $V_2O_5$(001) surface is physisorption, which supports the previous experimental identifications[7, 9, 10].

Furthermore, we also give the most stable $H_2O/V_2O_5$ interface structure (Fig. 4) after an optimization of various structures. We suggest whe the ratio of $H_2O$ and $V_2O_5$ is 1 (*i.e*, the same number of $H_2O$ molecule and $V_2O_5$ unit), $H_2O/V_2O_5$ interface structure can still maintain stable (a negative value relative to isolated $H_2O$ molecule). The adsorption energy for $H_2O$ in $H_2O/V_2O_5$ interface is –0.75 eV, where the negative energy means the adsorption is exothermic. The other $H_2O/V_2O_5$ interface structures are shown in Fig. S1. Fig. 4 shows that hydrogen binding interactions are generally found in $H_2O/V_2O_5$, which contributes to the stability of $H_2O/V_2O_5$ interface. More importantly, the right inset of Fig. 4 indicates the water forms a weakly ordered overlayer with $V_2O_5$(001) surface. Therefore, there is a locally ordered (2 × 2) superstructure of molecular water in $H_2O/V_2O_5$ interface. The formation of ordered overlayers has been observed on some oxide surfaces like $TiO_2$(101)[27].

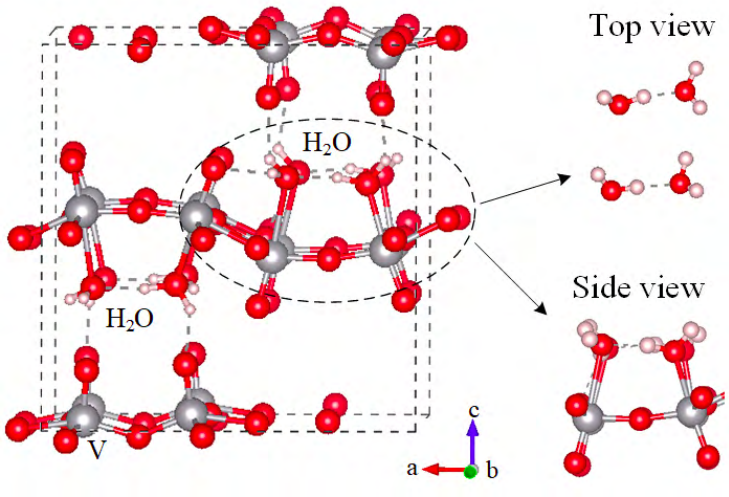


**Fig. 4. Scheme view of the most stable $H_2O/V_2O_5$ interface structure ($8{\cdot}H_2O/8{\cdot}V_2O_5$) (Red spheres are O atoms, gray spheres are V atoms, and dashed lines are hydrogen bonding interaction)**

To determine if the dissociation of $H_2O$ occurs on the $V_2O_5(001)$ surface, the partial dissociation of $H_2O$ is proposed, in which products are one hydroxyl group and one hydrogen atom. Hydrogen atom approaches different oxygen sites of the surface including O(1), O(2) and O(3) sites, and the hydroxyl group attaches to a V site, as shown in Fig. S2. The calculated adsorption energies for water dissociation at O(1), O(2) and O(3) sites displayed in Fig. S2 are positive with 171.73, 197.78 and 209.36 kJ/mol, suggesting that the three types of $H_2O$ dissociative adsorption are energetically unfavorable. Therefore, the dissociation of the water hardly occurs on the stoichiometric $V_2O_5(001)$ surface.

### 3. 2 Adsorption and dissociation of $H_2O$ on oxygen-vacancy $V_2O_5(001)$ surface

Oxygen-vacancies play an important role in catalytic reactions, and thus it is necessary to study the adsorption and dissociation of water on the oxygen-vacancy $V_2O_5(001)$ surface. Considering the interlayer interaction effect on the geometrical structure and electronic characterization of the oxygen-vacancy surface, a two-layer-slabs model was built, as shown in Fig. 5. In general, water prefers to interact with the surface atoms with high electron deficiency. Thereby, the favorable site for $H_2O$ adsorption is $V_{cus}$ (cus stands for one-fold coordinately unsaturated site). The optimized parameters for $H_2O$ adsorption on oxygen-vacancy surface are presented in Table 2.

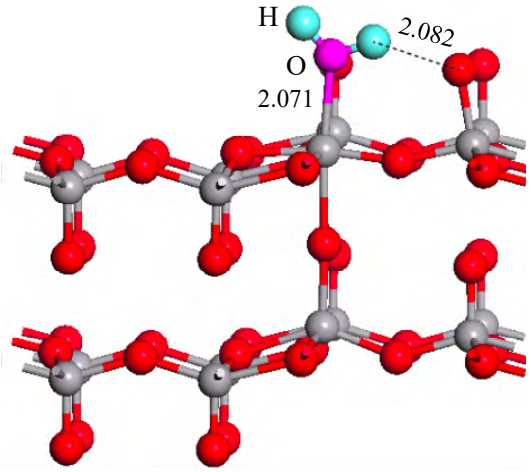


**Fig. 5. $H_2O$ adsorption on the V site of oxygen-vacancy $V_2O_5(001)$ surface (Red spheres: O atoms, gray spheres: V atoms, purple spheres: $O_w$ atoms of $H_2O$, and blue spheres: H atoms)**

**Table 2. Optimized Parameters for $H_2O$ Adsorption on the Oxygen-vacancy $V_2O_5(001)$, $V_2O_5(100)$ and $V_2O_5(010)$ Surfaces**

| Surfaces | $E_{ads}$ (kJ/mol) | $R_{V\text{-}Ow}$ (Å) | $R_{Ow\text{-}H}$ (Å) | $\theta_{H\text{-}Ow\text{-}H}$ (°) |
|---|---|---|---|---|
| Oxygen-vacancy $V_2O_5(001)$ | –98.41 | 2.071 | 0.981/1.091 | 110.3 |
| $V_2O_5(100)$ | –108.06 | 2.174 | 0.977/0.978 | 107.4 |
| $V_2O_5(010)$ | –84.90 | 2.275 | 0.980/0.991 | 106.1 |

$E_{ads}$, R and $\theta$ denote the adsorption energies, bond lengths and the angle of $H_2O$, respectively.

After adsorption, as shown in Fig. 5, the $H_2O$ is strongly adsorbed on the surface with an adsorption energy of –98.41 kJ/mol, forming two bonds: the $O_w$ atom of $H_2O$ forms a covalent bond with V atom with a distance of 2.071 Å, and one H atom generates a H-bond with surface O(1) atom with a distance of 2.082 Å. The strong H-bonding gives rise to a significant OH bond stretching with the O–H distance elongating from 0.973 to 1.091 Å, suggesting the bond is somewhat activated.

In addition, the dissociative chemisorption of $H_2O$ is investigated to understand the properties and reactivity of $H_2O$ on oxygen-vacancy $V_2O_5(001)$ surface. The strong adsorption of the pre-dissociation state of $H_2O$ allows the $O_w$–H bond to be activated, leading to the migration of H atom to the surface O atom to form an adatom and a hydroxyl species. Thus, the energy profile of water dissociation via $O_w$–H scission is examined and the intermediate, transition state, and final state (FS) along the pathway are also located, as shown in Fig. 6. Relative to the adsorption configuration, the dissociation of $H_2O$ is exothermic by 37.69 kJ/mol. The energy barrier is 93.72 kJ/mol, suggesting the dissociation might be difficult at low temperature. During the reaction process, the $O_w$–H bond length increases gradually: 1.091 Å in IM1, 1.501 Å in TS1, and finally breakes in FS1, indicating the $O_w$–H bond broken process. At the same time, the H–O(1) and $O_w$–V bond lengths reduce gradually: 2.082 and 2.071 Å in IM1, 1.620 and 1.970 Å in TS1, and 1.096 and 1.874 Å in FS1. The changes of bond lengths indicate H–O(1) and $O_w$–V are gradually strengthened.

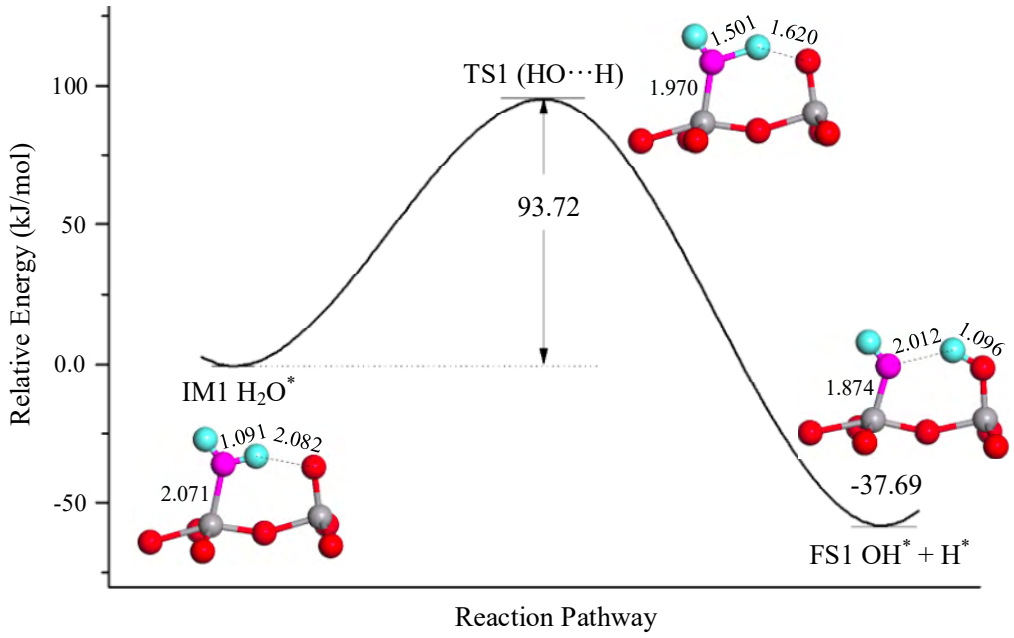


**Fig. 6. Energy profile for $H_2O$ dissociation on oxygen-vacancy $V_2O_5(001)$ surface with the relative intermediate, transition state and final state. The asterisks here denote the adsorption species (Red, gray, purple and blue spheres are O, V, $O_w$ of $H_2O$ and H atoms, respectivley)**

From the above analyses, $H_2O$ can undergo dissociative chemisorption on the oxygen-vacancy $V_2O_5(001)$ surface forming the surface hydroxyl group and adsorbed H atom, which is consistent with the experimental result that the lattice oxygen of $V_2O_5$ undergoes isotope exchange with the adsorbed water[11, 12]. In addition, $H_2O$ dissociative adsorption may alter the structures of $V_2O_5$ surface, thereby affecting the reactivity of $V_2O_5$-based catalysts and the redox cycle of $V_2O_5$-based heterogeneous reactions, which can be applied to guide the formation of surface lattice oxygen in isotope exchange experiments.

### 3. 3 Adsorption and dissociation of $H_2O$ on the $V_2O_5$ (010) and (100) surfaces

The side ((010) and (100) planes) surfaces contribute about 15% of the total surface area of a $V_2O_5$ crystallite, indicating a non-negligible role in the catalytic activity of $V_2O_5$[28]. Therefore, in this study, the adsorption and dissociation of water on the (010) and (100) planes are also studied.

The optimized parameters of water adsorption on the side $V_2O_5$ surfaces, i.e., $V_2O_5(100)$, $V_2O_5(010)$, are summarized in Table 2 and the optimized configurations are shown in Fig. 7a and 8a. In Table 2, the $H_2O$ is strongly adsorbed on the V sites of $V_2O_5(100)$ and (010) surfaces with the adsorption energies to be –108.06 and –84.90 kJ/mol and the V–$O_w$ bond lengths of 2.174 and 2.275 Å, respectively. In comparison with the adsorption energy of $H_2O$ on stoichiometric $V_2O_5(001)$ surface, molecular $H_2O$ adsorption on the side of $V_2O_5$ ((100) and (010)) surfaces is stronger than that on the stoichiometric $V_2O_5(001)$ surface, suggesting that the side $V_2O_5$ surfaces are chemically more active and may play an important role in the activity of $V_2O_5$ as an oxidation or reduction catalyst.

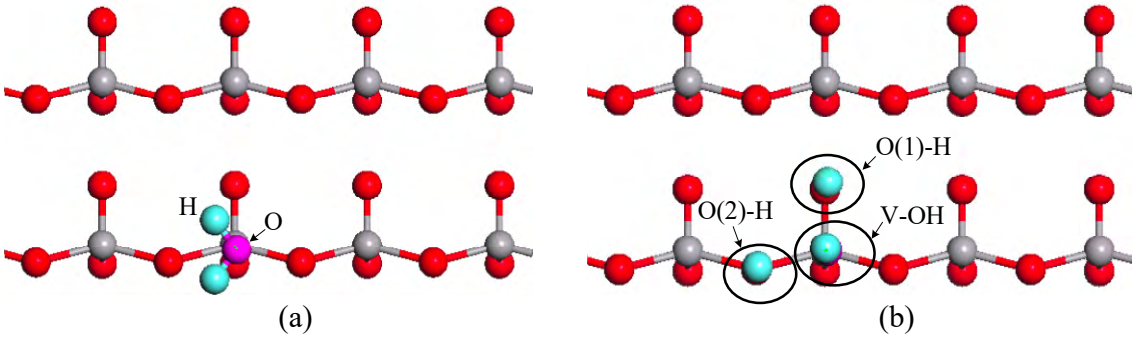


**Fig. 7. (a) Optimized structures of $H_2O$ adsorbed on the $V_2O_5(100)$ surface; (b) Possible dissociative types of $H_2O$ on the $V_2O_5(100)$ surface (Red spheres: O atoms, gray spheres: V atoms, purple spheres: $O_w$ atoms of $H_2O$, and blue spheres: H atoms)**

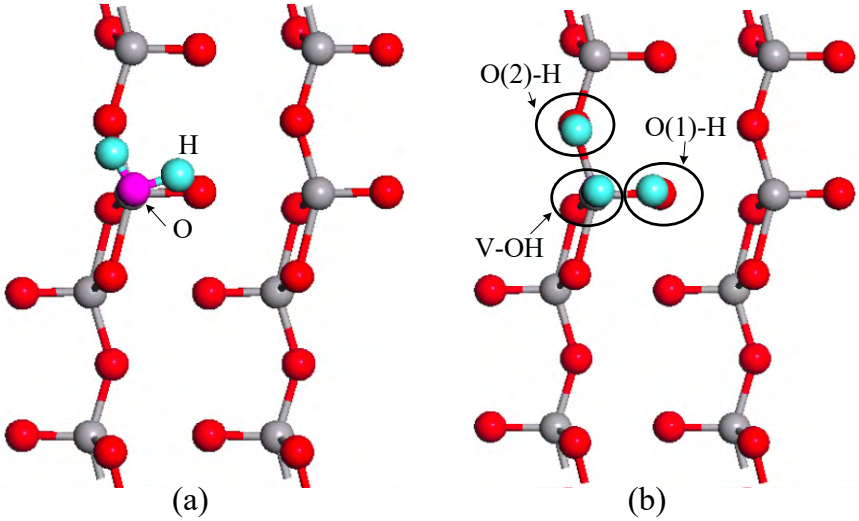


**Fig. 8. (a) Optimized structures of $H_2O$ adsorbed on $V_2O_5(010)$ surface; (b) Possible dissociative types of $H_2O$ on the $V_2O_5(010)$ surface (Red, gray, purple and blue spheres are O, V, $O_w$ of $H_2O$ and H atoms, respectivley)**

Next, the water dissociative chemisorption on the side $V_2O_5$ surfaces is investigated. The possible dissociative types of $H_2O$ on the side $V_2O_5$ surface are shown in Figs. 7b and 8b. The calculated energy profiles for (100) and (010) surfaces, along with intermediates, transition states and final states, are shown in Figs. 9 and 10, respectively.

For the $V_2O_5$(100) surface, two pathways are examined, i.e., IM2 → TS2 → FS2 and IM2 → TS3 → FS3, namely pathways A and B, as shown in Fig. 9. The energies of the optimized structures are relative to the intermediate. For pathway A, $H_2O$ adsorbs on the surface to form intermediate IM2, then the $O_w$–H bond is broken through the transition state TS2 to form FS2 with independently adsorbed hydroxyl group on the V site and H atom on the O(1) site. The reaction barrier is 71.50 kJ/mol and the process is exothermic by 41.56 kJ/mol. During the process, the $O_w$–H bond length increases gradually: 0.991 Å in IM2, 1.391 Å in TS2, and finally breaks in FS2, indicating the $O_w$–H bond broken process. At the same time, the H–O(1) and $O_w$–V bond lengths reduce gradually: 2.390 and 2.174 Å in IM2, 1.421 and 2.067 Å in TS2, and 0.978 and 1.840 Å in FS2. The changes of bond lengths suggest H–O(1) and $O_w$–V are gradually strengthened. For pathway B, the energy barrier is 78.25 kJ/mol, which is about 6.75 kJ/mol higher than that of pathway A. The reaction is exothermic by 22.32 kJ/mol which is smaller than that of pathway A (41.56 kJ/mol). These results indicate that pathway A is kinetically and thermodynamically more favored than pathway B. Furthermore, the energy barriers of pathways A and B are 71.50 and 78.25 kJ/mol, respectively. This difference should result from different calculated models and transition state searching methods.

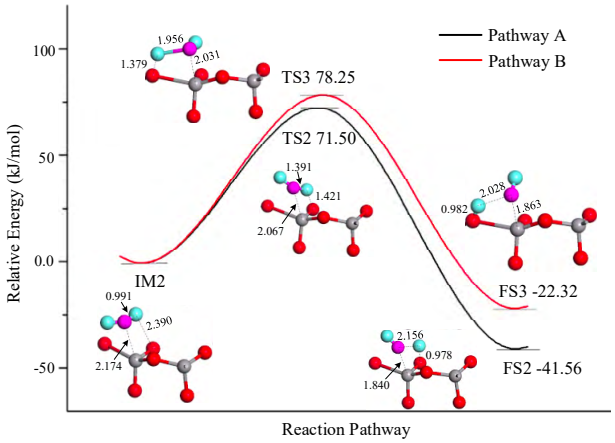


**Fig. 9. Energy profile for $H_2O$ dissociation on $V_2O_5$(100) surface with the relative intermediates, transition states and final states (Red spheres: O atoms, gray spheres: V atoms, purple spheres: $O_w$ atoms of $H_2O$, and blue spheres: H atoms)**

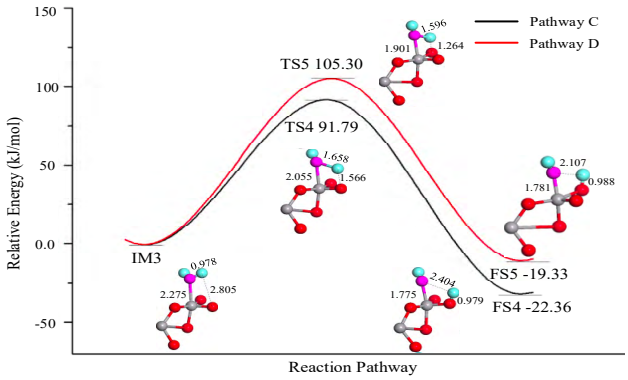


**Fig. 10. Energy profile for $H_2O$ dissociation on $V_2O_5$(010) surface with the relative intermediates, transition states and final state (Red, gray, purple and blue spheres are O, V, $O_w$ of $H_2O$ and H atoms, respectivley)**

In the same way, the energy profile of $H_2O$ dissociation on $V_2O_5(010)$ surface is also examined, as shown in Fig. 10. Two pathways are examined, i.e., IM3 → TS4 → FS4 and IM3 → TS5 → FS5, namely pathways C and D. For pathway C, the dissociation process is exothermic by 22.36 kJ/mol with an energy barrier of 91.79 kJ/mol, while for pathway D, the corrponding values are 19.33 and 105.30 kJ/mol, respectivley. Comparing the dissociation pathway of $H_2O$ on $V_2O_5(100)$ and $V_2O_5(010)$ surfaces found the $H_2O$ dissociation on $V_2O_5(100)$ surface is more favorable both thermodynamically and kinetically than that on the $V_2O_5(010)$ surface. Based on the above analyses, the side ((010) and (100) planes) $V_2O_5$ surfaces are more active than the stoichiometric $V_2O_5(001)$ one for $H_2O$ adsorption and dissociation, which suggests that $V_2O_5(100)$ and (010) surfaces show more strong reactivity for surface reactions.

## 4 CONCLUSION

The water/$V_2O_5$ interface, adsorption and dissociation of $H_2O$ on different $V_2O_5$ surfaces are investigated using periodic density functional method. Adsorption of $H_2O$ on stoichiometric $V_2O_5(001)$ surface follows the physisorption mechanism and the dissociation of $H_2O$ hardly occurs due to the thermodynamic analysis. The most stable $H_2O/V_2O_5$ interface structure shows that $H_2O$ adsorbs as an intact monomer with a locally ordered superstructure of molecular water. On the oxygen-vacancy $V_2O_5(001)$ surface, $H_2O$ is strongly adsorbed on V site and can undergo dissociative chemisorption with a moderate energy barrier, forming a surface hydroxyl and a H adatom. For (100) and (010) of $V_2O_5$ surfaces, $H_2O$ is also strongly adsorbed on both surfaces. The energy profile analyses show that $H_2O$ can undergo dissociative chemisorption with low energy barriers, indicating (100) and (010) surfaces are more active than the $V_2O_5(001)$ surface. The formation of O–V bond from the hydroxyl group adsorbed on V sites on oxygen-vacancy $V_2O_5(001)$ and side $V_2O_5$ surfaces suggests that $V_2O_5$ catalysts can take the oxygen from $H_2O$, which is consistent with the experimental results that the lattice oxygen of $V_2O_5$ undergoes isotope exchange with that of $H_2O$.

**Conflicts of interest:** The authors declare no conflict of interest.

## REFERENCES

(1) Verdaguer, A.; Sacha, G. M.; Bluhm, H.; Salmeron, M. Molecular structure of water at interfaces: wetting at the nanometer scale. *Chem. Rev.* **2006**, 106, 1478–1510.

(2) Henderson, M. A. The interaction of water with solid surfaces: fundamental aspects revisited. *Surf. Sci. Rep.* **2002**, 46, 1–308.

(3) Fujishima, A.; Honda, K. Electrochemical photolysis of water at a semiconductor electrode. *Nature* **1972**, 238, 37–38.

(4) Chen, X.; Wang, L.; Li, H.; Cheng, F.; Chen, J. Porous $V_2O_5$ nanofibers as cathode materials for rechargeable aqueous zinc-ion batteries. *J. Energy Chem.* **2019**, 38, 20–25.

(5) Geng, H.; Cheng, M.; Wang, B.; Yang, Y.; Zhang, Y.; Li, C. C. Electronic structure regulation of layered vanadium oxide via interlayer doping strategy toward superior high-rate and low-temperature zinc-ion batteries. *Adv. Funct. Mater.* **2019**, 1907684.

(6) Zhang, B.; Liu, J.; Dai, G.; Chang, M.; Zheng, C. Insights into the mechanism of heterogeneous mercury oxidation by HCl over $V_2O_5/TiO_2$ catalyst: periodic density functional theory study. *P. Combust. Inst.* **2015**, 35, 2855–2865.

(7) Busca, G.; Ramis, G.; Lorenzelli, V. FT-IR study of the surface properties of polycrystalline vanadia. *J. Mol. Catal.* **1989**, 50, 231–240.

(8) Topsøe, N. Y. Characterization of the nature of surface sites on vanadia-titania catalysts by FTIR. *J. Catal.* **1991**, 128, 499–511.

(9) Costa, A. D.; Mathieu, C.; Barbaux, Y.; Poelman, H.; Dalmai-Vennik, G.; Fiermans, L. Observation of the $V_2O_5(001)$ surface using ambient atomic force microscopy. *Surf. Sci.* **1997**, 370, 339–344.

(10) Moshfegh, A. Z.; Ignatiev, A. A temperature programmed desorption study of the $H_2O/V_2O_5$ system. *Surf. Sci.* **1992**, 275, L650–L654.

(11) Sadovskaya, E. M.; Goncharov, V. B.; Gulyaeva, Y. K.; Popova, G. Y.; Andrushkevich, T. V. Kinetics of the $H_2{}^{18}O/H_2{}^{16}O$ isotope exchange over vanadia-titania catalyst. *J. Mol. Catal. A: Chem.* **2010**, 316, 118–125.

(12) Lee, E. L.; Wachs, I. E. In situ raman spectroscopy of $SiO_2$-supported transition metal oxide catalysts: an isotopic $^{18}O–^{16}O$ exchange study. *J. Phys. Chem. C* **2008**, 112, 6487–6498.

(13) Ma, J. B.; Zhao, Y. X.; He, S. G.; Ding, X. L. Experimental and theoretical study of the reactions between vanadium oxide cluster cations and water. *J. Phys. Chem. A* **2012**, 116, 2049–2054.

(14) Goclon, J.; Grybos, R.; Witko, M.; Hafner, J. Oxygen vacancy formation on clean and hydroxylated low-index $V_2O_5$ surfaces: a density functional investigation. *Phys. Rev. B* **2009**, 79, 075439.

(15) Yin, X.; Fahmi, A.; Han, H.; Endou, A.; Ammal, S. S. C.; Kubo, M.; Teraishi, K.; Miyamoto, A. Adsorption of $H_2O$ on the $V_2O_5$(010) surface studied by periodic density functional calculations. *J. Phys. Chem. B* **1999**, 103, 3218–3224.

(16) Hejduk, P.; Szaleniec, M.; Witko, M. Molecular and dissociative adsorption of water at low-index $V_2O_5$ surfaces: DFT studies using cluster surface models. *J. Mol. Catal. A: Chem.* **2010**, 325, 98–104.

(17) Segall, M. D.; Lindan, P. J. D.; Probert, M. J.; Pickard, C. J.; Hasnip, P. J.; Clark, S. J.; Payne, M. C. First-principles simulation: ideas, illustrations and the CASTEP code. *J. Phys.: Condens. Matter.* **2002**, 14, 2717–2744.

(18) Perdew, J. P.; Burke, K.; Ernzerhof, M. Generalized gradient approximation made simple. *Phys. Rev. Lett.* **1996**, 77, 3865–3868.

(19) Perdew, J. P.; Burke, K.; Wang, Y. Generalized gradient approximation for the exchange-correlation hole of a many-electron system. *Phys. Rev. B* **1996**, 54, 16533–16539.

(20) Vanderbilt, D. Soft self-consistent pseudopotentials in a generalized eigenvalue formalism. *Phys. Rev. B* **1990**, 41, 7892–7895.

(21) Chadi, D. J. Special points for Brillouin-zone integrations. *Phys. Rev. B* **1977**, 16, 1746–1747.

(22) Enjalbert, R.; Galy, J. A refinement of the structure of $V_2O_5$. *Acta Crystallogr., Sect. C.* **1986**, 42, 1467–1469.

(23) Halgren, T. A.; Lipscomb, W. N. The synchronous-transit method for determining reaction pathways and locating molecular transition states. *Chem. Phys. Lett.* **1977**, 49, 225–232.

(24) Zhang, B.; Liu, J.; Shen, F. Heterogeneous mercury oxidation by HCl over $CeO_2$ catalyst: density functional theory study. *J. Phys. Chem. C* **2015**, 119, 15047–15055.

(25) Zhang, B.; Liu, J.; Yang, Y.; Chang, M. Oxidation mechanism of elemental mercury by HCl over $MnO_2$ catalyst: insights from first principles. *Chem. Eng. J.* **2015**, 280, 354–362.

(26) Ranea, V. A.; Vicente, J. L.; Mola, E. E.; Uyewa Mananu, R. A theoretical study of water chemisorption on the (001) plane of $V_2O_5$. *Surf. Sci.* **1999**, 442, 498–506.

(27) He, Y.; Tilocca, A.; Dulub, O.; Selloni, A.; Diebold, U. Local ordering and electronic signatures of submonolayer water on anatase $TiO_2$(101). *Nat Mater.* **2009**, 8, 585–589.

(28) Goclon, J.; Grybos, R.; Witko, M.; Hafner, J. Relative stability of low-index $V_2O_5$ surfaces: a density functional investigation. *J. Phys.: Condens. Matter.* **2009**, 21, 095008.